Constraining the SMEFT top sector through searches in $t\bar{t}Z$ and tZj with Machine Learning

Rahool Barman
Oklahoma State University

In Collaboration with:
Dr. Ahmed Ismail (Oklahoma State Univ.)

(in preparation)

IMEPNP 2022
IOP Bhubaneswar

February 7 - 12, 2022

The SMEFT framework

- Implications from Heavy BSM physics on lower scales can be parameterized through higher dimensional effective operators.
- Provides a model-independent way of parameterizing the deviations from the SM,

$$\mathcal{L}_{SMEFT} = \mathcal{L}_{SM} + \sum_i \frac{\mathcal{C}_i}{\Lambda^2}\mathcal{O}_i^{(6)} + \mathcal{O}\left(\Lambda^{-4}\right).$$

- $\mathcal{C}_i$ free parameters by definition and are constrained by experimental measurements.
- Typically, a dim-6 operator $\{\mathcal{O}_i^{(6)}\}$ results in the following modifications to any measured observable $\mathcal{X}$,

$$\mathcal{X} = \mathcal{X}_{SM} + \sum_i \mathcal{X}_i' \frac{\mathcal{C}_i^{(6)}}{\Lambda^2} + \sum_{i,j} \mathcal{X}_i'' \frac{\mathcal{C}_i^{(6)}\mathcal{C}_j^{(6)}}{\Lambda^4},$$

SMEFT in top sector

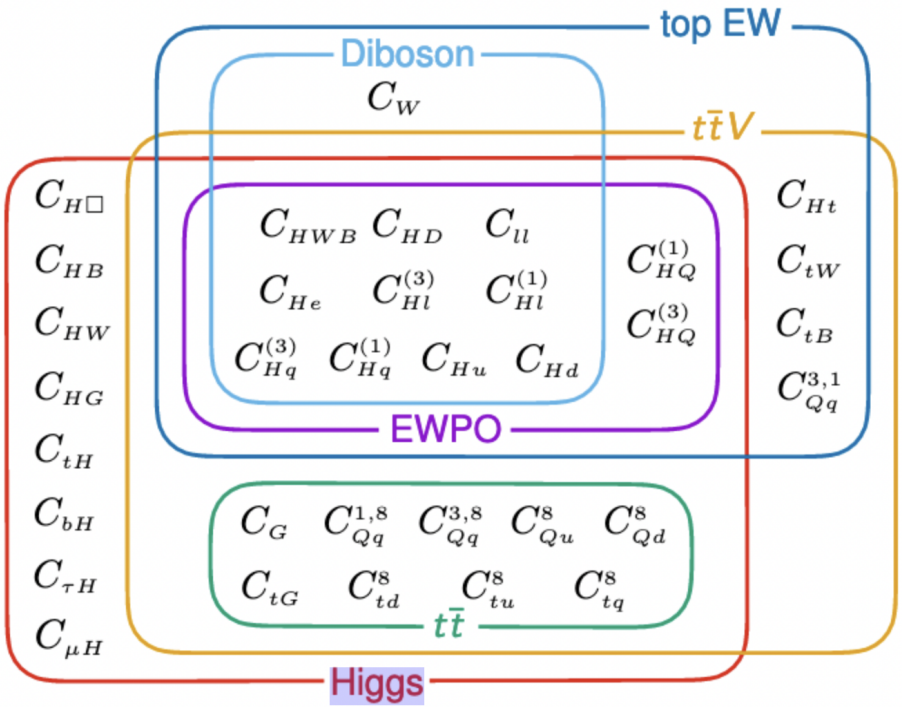

[Ellis, Madigan, Mimasu, Sanz, You (2020)]

- Operators that directly modify the coupling of top-quark with SM fields:
  - $\{$4 heavy quark$\}$ operators $\rightarrow$ constrained by $t\bar{t}t\bar{t}$, $t\bar{t}b\bar{b}$.
  - $\{$2 heavy 2 light quark$\}$ operators $\rightarrow$ constrained by $t\bar{t}$ and $t\bar{t}V$.
  - $\{$2 heavy quarks and bosonic fields, including H $\}$ $\rightarrow$ constrained by t, tV, $t\bar{t}V$).

SMEFT in top sector

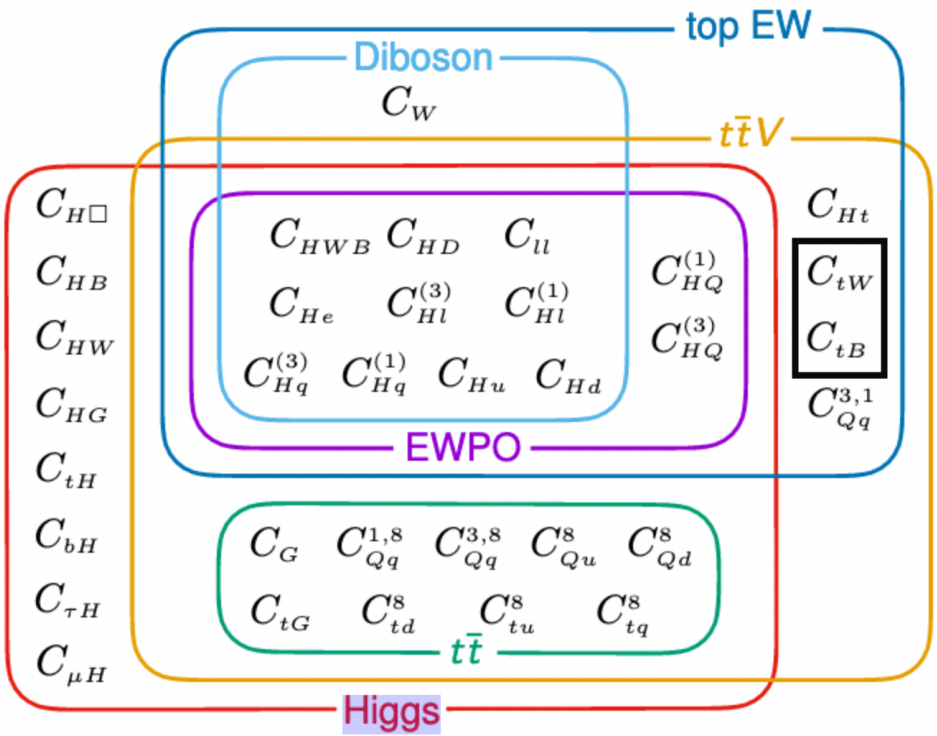

[Ellis, Madigan, Mimasu, Sanz, You (2020)]

- Operators that directly modify the coupling of top-quark with SM fields:
  - $\{4$ heavy quark$\}$ operators $\rightarrow$ constrained by $t\bar{t}t\bar{t}$, $t\bar{t}b\bar{b}$.
  - $\{2$ heavy 2 light quark$\}$ operators $\rightarrow$ constrained by $t\bar{t}$ and $t\bar{t}V$.
  - $\{2$ heavy quarks and bosonic fields, including H $\}$ $\rightarrow$ constrained by t, tV, $t\bar{t}V$).

$\mathcal{O}_{tZ}$ and $\mathcal{O}_{tW}$

- $\mathcal{O}_{tW} = \left(\bar{Q}_3 \sigma^{\mu\nu} U_3\right) \tau^a \tilde{H} W^a_{\mu\nu}$
  Constrained mainly by:
  - W helicity fraction measurements in $t\bar{t}$ data.
  - single top and tV measurements.

- $O_{tB} = \left(\bar{Q}_3 \sigma^{\mu\nu} U_3\right) \tilde{H} B_{\mu\nu}$

$\rightarrow \mathcal{O}_{tZ} = -\sin\theta_W \mathcal{O}_{tB} + \cos\theta_W \mathcal{O}_{tW}$

Constrained by:
- $t\bar{t}Z$ and $t\bar{t}\gamma$ measurements.
- tV measurements.

[CMS; arXiv: 1907.11270]

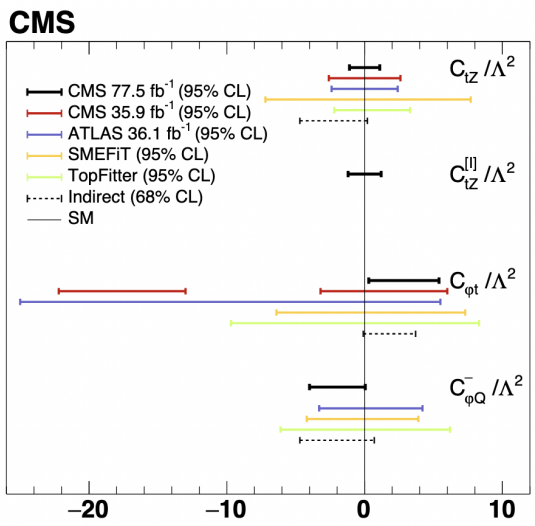

$\rightarrow$ considerable deviations in the tail of diff. distributions
[Degrande, Maltoni, Mimasu, Vryonidou, Zhang (2018)]

$\rightarrow$ inclusion of differential measurements might lead to improvement in sensitivity.

- With improved statistics, HL-LHC would be an ideal testbed for such measurements.

With shape information at our disposal, how well can we constrain $\mathcal{O}_{tZ}$ and $\mathcal{O}_{tW}$ at the HL-LHC?

Global-fit: $\mathcal{O}_{tW}$: [-0.241,0.086],

$\mathcal{O}_{tZ}$: [-1.129,0.856]
[Ethier, Magni, Maltoni, Mantani, Nocera, Rojo, Slade, Vryonidou, Zhang (2021)]

Goal

The goal of this work: evaluate the projected capability of the HL-LHC in probing $\mathcal{O}_{tW}$ and $\mathcal{O}_{tZ}$ through searches in $t\bar{t}Z$ and tZj channels, while including kinematic information.

- We focus on:
  - $t\bar{t}Z \to 3\ell + 2b + \geq 2\ j$
  - $tZj \to 3\ell + 1b + 1/2\ j$
- Both channels allow the testing of top-quark NC which are not accessible through top decay.
- NP effect in both production and decay are considered,
  $\to \mathcal{O}_{tZ}$ can affect only production
  $\to \mathcal{O}_{tW}$ can affect both production and decay.
- Each channel is analyzed with :
  1. Conventional cut-and-count approach.
  2. Multivariate analysis with Deep Neural Network.
  3. likelihood-free inference using `MadMiner`.

$pp \to t\bar{t}Z$ channel

- We focus on:
  $t\bar{t}Z \to (t \to \ell\nu b)(\bar{t} \to jj\bar{b})(Z \to \ell\ell)$

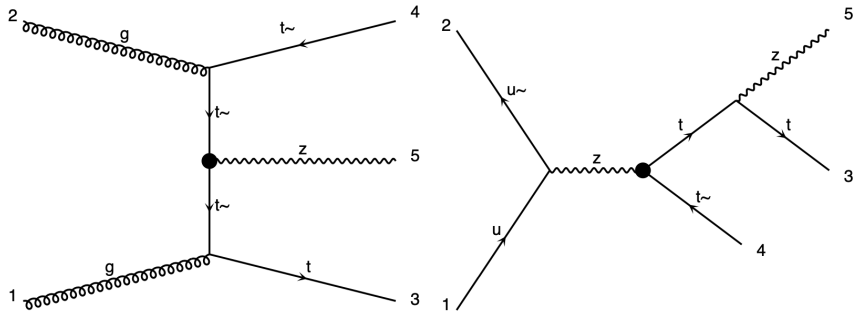

- Backgrounds: SM $t\bar{t}Z$, $WZ + jets$, tWZ, $t\bar{t}\gamma$, $t\bar{t}h$, VVV.
- NP modifications in tWZ are also taken into account.

Event selection

- Final state: 3 ℓ + 2 b jets + $\geq$ 2 j
- SFOS-ℓ pair with $m_{\ell\ell} = m_Z \pm 10$ GeV.
- $\not{p}_z$ computed by constraining $m_{\ell_W \nu} = m_W$.
- top reconstructed by minimizing: $\left(m_{jjb} - m_t\right)^2 + (m_{\ell\nu b} - m_t)^2$.

Reconstructed observables:

$$p_{T,\alpha}, \eta_\alpha, \phi_\alpha \{\alpha = \alpha_Z, \alpha_{t_\ell}, \alpha_{t_h}, t_\ell, t_h, Z\}, \{\alpha_Z = \ell_1, \ell_2;\ \alpha_{t_\ell} = \ell_W, \nu_t, b_{t_\ell};\ \alpha_{t_h} = j_{1t}, j_{2t}, b_{t_h}\}$$

$$\Delta\phi_{\beta\epsilon}, \Delta\eta_{\beta\epsilon} \{\beta, \epsilon = \alpha_Z, \alpha_{t_\ell}, \alpha_{t_h}, t_\ell, t_h, Z; \beta \neq \epsilon\}, \theta^{\star t\bar{t}Z}_{\alpha_Z}, \theta^{\star t\bar{t}Z}_{t_\ell}, \theta^{\star t\bar{t}Z}_{t_h}, \theta^{\star t\bar{t}}_{t_\ell}, \theta^{\star t\bar{t}}_{t_h},$$

$$p_{T,t_\ell Z}, p_{T,t_h Z}, p_{T,t_\ell t_h}, p_{T,t_\ell t_h Z}, H_T, m_{t_\ell}, m_{t_h}, m_Z, m_{t_\ell Z}, m_{t_h Z}, m_{t_\ell t_h}, m_{t_\ell t_h Z}, m_{T,l_W},$$

$$\Delta R^{\min}_{\ell\ell}, \Delta R^{\max}_{\ell\ell}, \Delta R^{\min}_{\ell b}, \Delta R^{\max}_{\ell b}.$$

Cut-based optimization

$\mathcal{O}_{tZ}$: Cut-and-count analysis performed at $\{\mathcal{O}_{tZ} = \pm 0.5, \pm 1.0, \pm 1.5, \pm 2.0\}$.

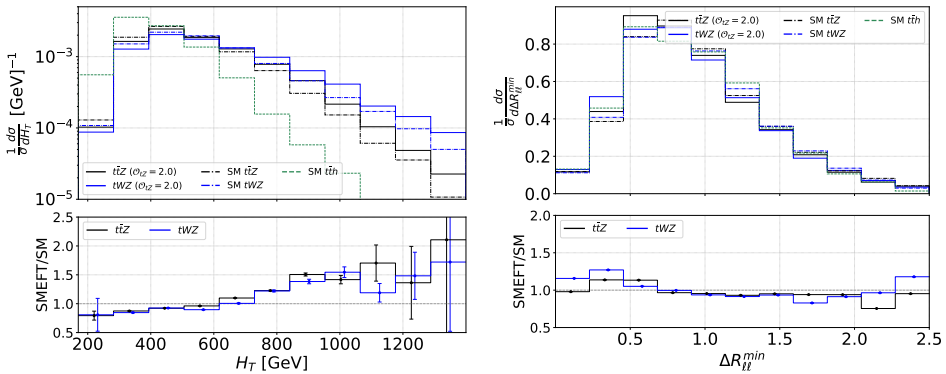

	$\mathcal{C}_{tZ} = 2.0$			$\mathcal{C}_{tZ} = -0.5$			
Event rates @ HL-LHC	$m_{t_hZ} >$ 250 GeV	$H_T >$ 300 GeV	$\Delta R_{\ell\ell}^{\min} <$ 2.75	$m_{t_hZ} >$ 350 GeV	$H_T >$ 650 GeV	$\Delta R_{\ell\ell}^{\min} <$ 2	$\Delta\phi_{\ell_W t_\ell} <$ 0.4
SMEFT $t\bar{t}Z$	2664	2611	2609	1489	419	411	215
SMEFT tWZ	151	149	148	103	38.1	37.1	17.5
$t\bar{t}Z$	1853	1800	1796	1442	392	381	185
tWZ	118	115	115	101.8	36.5	35.7	16.9
WZ	153	147	147	150	32.7	32.7	21.8
$t\bar{t}h$	14.1	12.8	12.8	8.4	0.82	0.81	0.26
$t\bar{t}\gamma$	19.7	18.9	18.9	15.1	3.7	3.6	1.6
Significance	18.17	18.47	18.51	1.16	1.32	1.47	2.04

$$\sigma_s^{NP} = (S_{SMEFT} - S_{SM})/\sqrt{S_{SM}}$$

$\mathcal{O}_{tW}$: Cut-and-count analysis performed at $\{\mathcal{O}_{tW} = \pm 0.24, \pm 0.48, \pm 0.72\}$.

	$\mathcal{C}_{tW} = 0.48$		$\mathcal{C}_{tW} = -0.48$		
Optimized cuts	H_T > 250 GeV	$\Delta R_{\ell b}^{\min} <$ 2.75	$\theta^{\star}_{\ell_2^{t\bar{t}Z}}$ [0.2 : 2.94]	$H_T >$ 250	$\Delta R_{\ell b}^{\min} <$ 2.5
SMEFT $t\bar{t}Z$	2210	2201	1616	1613	1593
SMEFT tWZ	131	129	125	124	121
$t\bar{t}Z$	1889	1881	1852	1849	1828
tWZ	122	121	119	119	115
WZ	150	136	142	139	125
$t\bar{t}h$	14.6	14.6	14.6	14.4	14.4
$t\bar{t}\gamma$	19.8	19.8	19.4	19.3	19.1
Significance	7.04	7.06	4.97	4.98	5.01

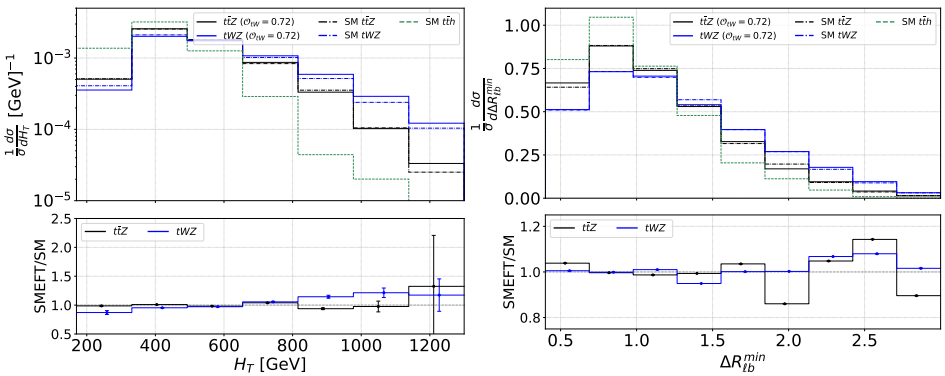

DNN setup

Why Deep Neural Network?

- Cut-based approach is relatively ineffective in exploring correlations among observables.
- becomes progressively cumbersome as the dimensionality of observables is increased.

$\rightarrow$ We construct a fully connected neural network using Keras with 150 observables.

Training dataset:

Signal: $t\bar{t}Z$ and tWZ events with at least one EFT vertex at production level.

Background: SM $t\bar{t}Z$, tWZ, $WZ + jets$

Test dataset:

SM(+)EFT $t\bar{t}Z$ and tWZ events with NP at production and decay, and SM $t\bar{t}Z$, tWZ, $WZ + jets$, $t\bar{t}\gamma$, $t\bar{t}h$.

DNN with 150 observables									
$\mathcal{C}_{tZ}$	SMEFT		Background					α	σ_S^{NP}
	$t\bar{t}Z$	tWZ	$t\bar{t}Z$	tWZ	WZ	$t\bar{t}h$	$t\bar{t}\gamma$		
2.0	1557	84.5	942	58.6	73.6	1.9	7.7	0.60	19.23
1.5	979	56.9	673	44.5	51.8	0.9	5.9	0.64	11.22
-0.5	1038	63.7	963	61.8	81.8	7.0	9.8	0.56	2.3
-2.0	2016	111	1258	82.9	114.5	4.3	11.8	0.55	20.18

- Overall, DNN for $\mathcal{O}_{tZ}$ showcases $\sim$ 5-10% improvement over cut-based.
- DNN for $\mathcal{O}_{tW}$ leads to a projected sensitivity that is comparable to that from cut-based.

Most-sensitive observables are identified through permutation feature importance scores.

35 most important observables:

- Invariant masses: $m_{t_\ell t_h}$, $m_{t_{\ell/h}Z}$, $m_{t_\ell t_h Z}$,
- Transverse momentum: H_T, $p_{T,\ell_{1/2}}$, p_{T,ℓ_W}, p_{T,b_h}, $p_{T,Z}$, $p_{T,t_{\ell/h}}$, $p_{T,t_{\ell/h}Z}$, $p_{T,t_\ell t_h}$,
- ΔR: $\Delta R_{\ell\ell}^{\min/\max}$, $\Delta R_{\ell b}^{\min}$,
- Azimuthal angles: ϕ_{ℓ_W}, ϕ_{t_ℓ}, $\Delta\phi_{\ell_W t_\ell}$, $\Delta\phi_{\ell_W \ell_1}$, $\Delta\phi_{\nu\ell_1}$, $\Delta\phi_{\nu b_2}$, $\Delta\phi_{b_\ell \ell_{1/2}}$, $\Delta\phi_{j_2\ell_1}$, $\Delta\phi_{b_h\ell_2}$, $\Delta\phi_{\ell_1 t_\ell}$,
- Pseudorapidities: η_{ℓ_1}, $\Delta\eta_{t_\ell Z}$, $\Delta\eta_{\nu Z}$, $\Delta\eta_{\ell_W\ell_2}$, $\Delta\eta_{b_\ell\ell_2}$, $\Delta\eta_{\ell_2 Z}$.
- DNN with these 35 observables leads to comparable sensitivity.

DNN with 150 observables									
$\mathcal{C}_{tZ}$	SMEFT		Background					α	σ_S^{NP}
	$t\bar{t}Z$	tWZ	$t\bar{t}Z$	tWZ	WZ	$t\bar{t}h$	$t\bar{t}\gamma$		
2.0	1557	84.5	942	58.6	73.6	1.9	7.7	0.60	19.23
1.5	979	56.9	673	44.5	51.8	0.9	5.9	0.64	11.22
-0.5	1038	63.7	963	61.8	81.8	7.0	9.8	0.56	2.3
-2.0	2016	111	1258	82.9	114.5	4.3	11.8	0.55	20.18

- Overall, DNN for $\mathcal{O}_{tZ}$ showcases $\sim$ 5-10% improvement over cut-based.
- DNN for $\mathcal{O}_{tW}$ leads to a projected sensitivity that is comparable to that from cut-based.

Most-sensitive observables are identified through permutation feature importance scores.

35 most important observables:

- Invariant masses: $m_{t_\ell t_h}$, $m_{t_{\ell/h}Z}$, $m_{t_\ell t_h Z}$,
- Transverse momentum: H_T, $p_{T,\ell_{1/2}}$, p_{T,ℓ_W}, p_{T,b_h}, $p_{T,Z}$, $p_{T,t_{\ell/h}}$, $p_{T,t_{\ell/h}Z}$, $p_{T,t_\ell t_h}$,
- ΔR: $\Delta R_{\ell\ell}^{\min/\max}$, $\Delta R_{\ell b}^{\min}$,
- Azimuthal angles: ϕ_{ℓ_W}, ϕ_{t_ℓ}, $\Delta\phi_{\ell_W t_\ell}$, $\Delta\phi_{\ell_W \ell_1}$, $\Delta\phi_{\nu\ell_1}$, $\Delta\phi_{\nu b_2}$, $\Delta\phi_{b_\ell \ell_{1/\ell_2}}$, $\Delta\phi_{j_2\ell_1}$, $\Delta\phi_{b_h\ell_2}$, $\Delta\phi_{\ell_1 t_\ell}$,
- Pseudorapidities: η_{ℓ_1}, $\Delta\eta_{t_\ell Z}$, $\Delta\eta_{\nu Z}$, $\Delta\eta_{\ell_W \ell_2}$, $\Delta\eta_{b_\ell \ell_2}$, $\Delta\eta_{\ell_2 Z}$.
- DNN with these 35 observables leads to comparable sensitivity.

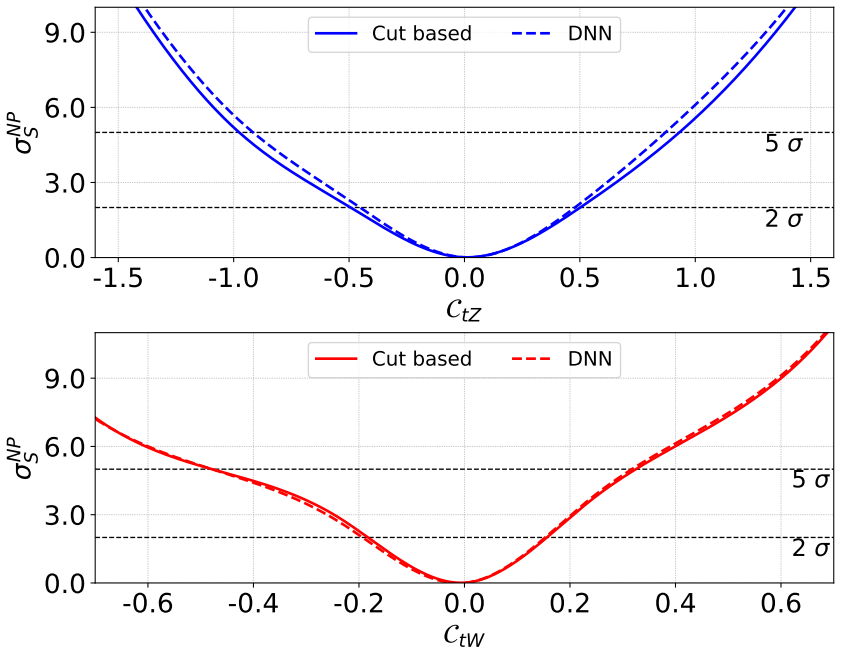

DNN with 150 observables									
$\mathcal{C}_{tZ}$	SMEFT		Background					α	σ_S^{NP}
	$t\bar{t}Z$	tWZ	$t\bar{t}Z$	tWZ	WZ	$t\bar{t}h$	$t\bar{t}\gamma$		
2.0	1557	84.5	942	58.6	73.6	1.9	7.7	0.60	19.23
1.5	979	56.9	673	44.5	51.8	0.9	5.9	0.64	11.22
-0.5	1038	63.7	963	61.8	81.8	7.0	9.8	0.56	2.3
-2.0	2016	111	1258	82.9	114.5	4.3	11.8	0.55	20.18

- Overall, DNN for $\mathcal{O}_{tZ}$ showcases $\sim$ 5-10% improvement over cut-based.
- DNN for $\mathcal{O}_{tW}$ leads to a projected sensitivity that is comparable to that from cut-based.

Most-sensitive observables are identified through permutation feature importance scores.

35 most important observables:

- Invariant masses: $m_{t_\ell t_h}$, $m_{t_{\ell/h}Z}$, $m_{t_\ell t_h Z}$,
- Transverse momentum: H_T, $p_{T,\ell_{1/2}}$, p_{T,ℓ_W}, p_{T,b_h}, $p_{T,Z}$, $p_{T,t_{\ell/h}}$, $p_{T,t_{\ell/h}Z}$, $p_{T,t_\ell t_h}$,
- ΔR: $\Delta R_{\ell\ell}^{\min/\max}$, $\Delta R_{\ell b}^{\min}$,
- Azimuthal angles: ϕ_{ℓ_W}, ϕ_{t_ℓ}, $\Delta\phi_{\ell_W t_\ell}$, $\Delta\phi_{\ell_W \ell_1}$, $\Delta\phi_{\nu\ell_1}$, $\Delta\phi_{\nu b_2}$, $\Delta\phi_{b_\ell \ell_{1/\ell_2}}$, $\Delta\phi_{j_2\ell_1}$, $\Delta\phi_{b_h\ell_2}$, $\Delta\phi_{\ell_1 t_\ell}$,
- Pseudorapidities: η_{ℓ_1}, $\Delta\eta_{t_\ell Z}$, $\Delta\eta_{\nu Z}$, $\Delta\eta_{\ell_W \ell_2}$, $\Delta\eta_{b_\ell \ell_2}$, $\Delta\eta_{\ell_2 Z}$.
- DNN with these 35 observables leads to comparable sensitivity.

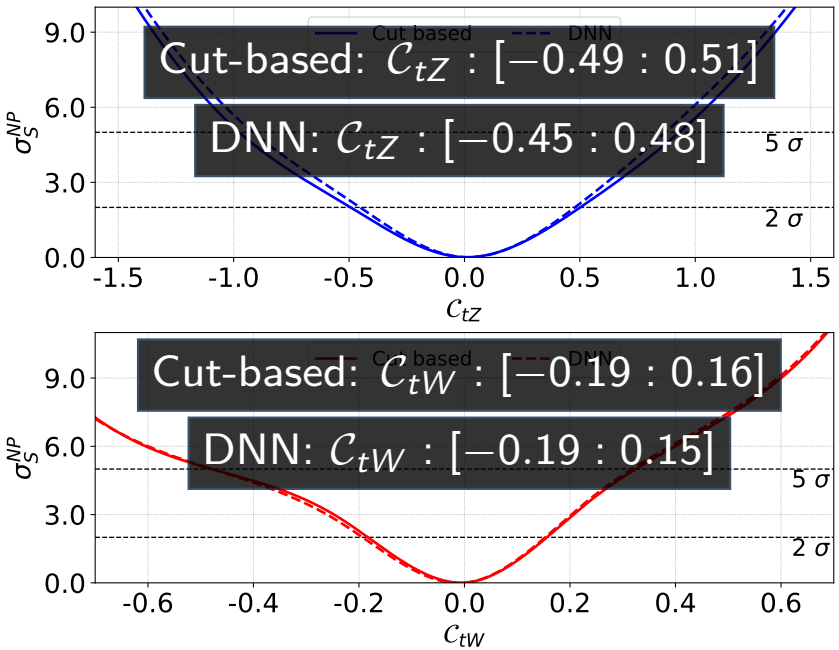

DNN

- Disparity between training and test dataset in DNN:
  - training data has no NP in top decay.
  - test dataset includes NP at production as well as decay.
- For consistency check, we also estimate projected sensitivities using **MadMiner**.

- Overall, DNN for $\mathcal{O}_{tZ}$ showcases $\sim$ 5-10% improvement over cut-based.
- DNN for $\mathcal{O}_{tW}$ leads to a projected sensitivity that is comparable to that from cut-based.

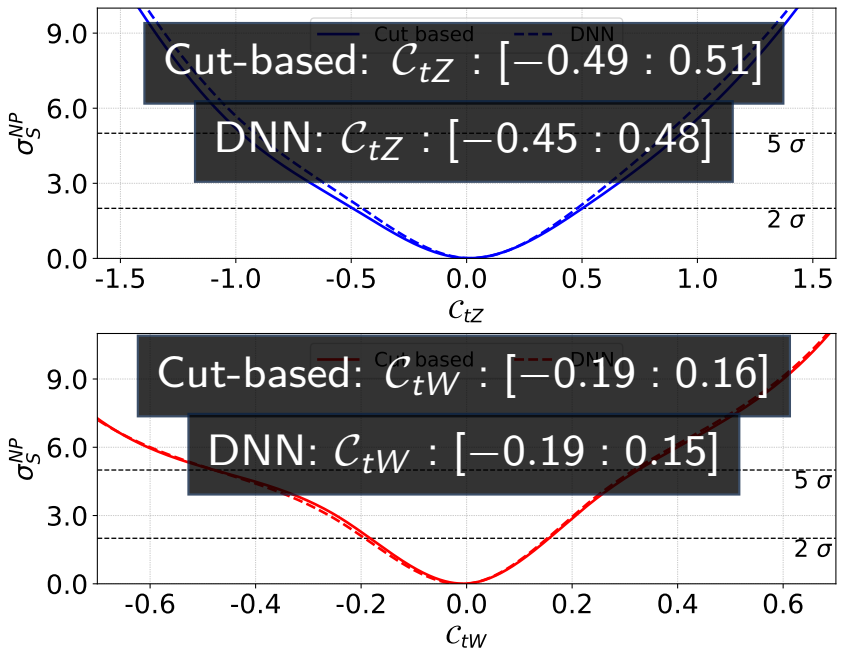

MadMiner

- A likelihood-based approach is followed to interpret the results
  $\rightarrow$ likelihood ratio $r(x|\theta, \theta_{SM})$ has been known as an excellent test statistic to discriminate NP effects parameterized by $\theta = (C_{tZ}, C_{tW})$ from SM $\theta_{SM} = (0, 0)$.
- At detector level, $r(x|\theta, \theta_{SM})$ cannot be computed directly, however, can be estimated through simulations.
- MadMiner resolves this intractability by employing ML based inference techniques. [Brehmer, Kling, Espejo, Cranner (2019)]

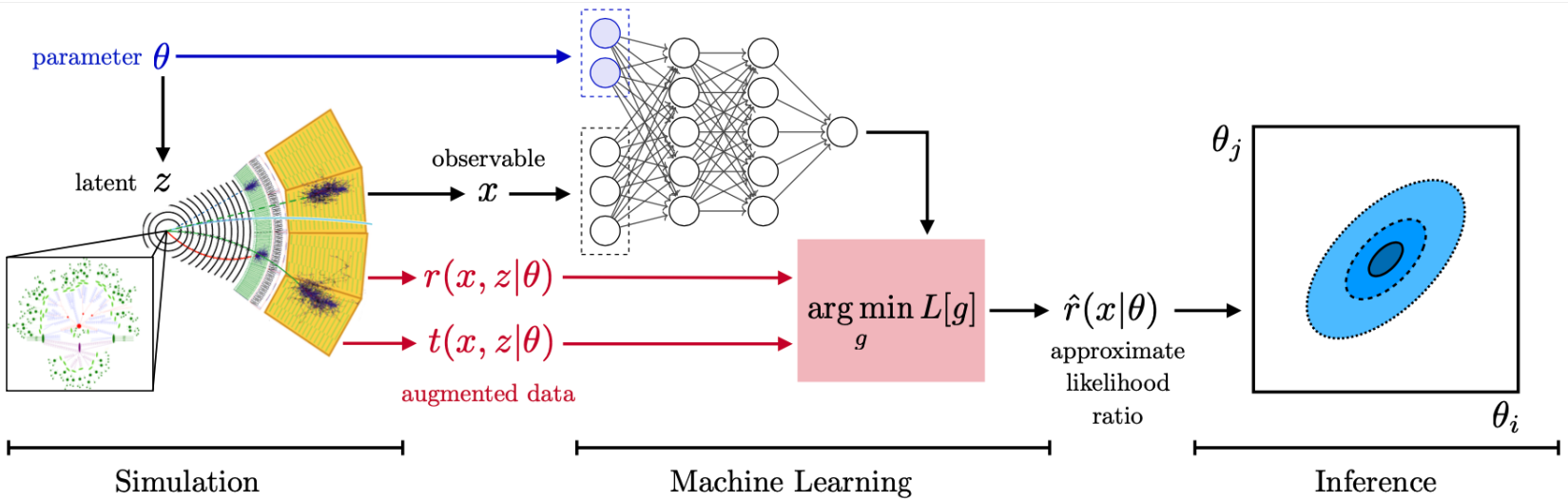

(taken from [Brehmer, Cranner, Louppe, Pavez (2018)])

MadMiner

- Interpolates matrix element (ME) information from MC simulated events as a function of θ.
- reconstructed observables x + ME information are used to train neural networks
  $\rightarrow$ accounts for parton shower, hadronization and detector effects.
- The joint likelihood ratio, $r(x, z|\theta_0, \theta_1) = p(x, z|\theta_0)/p(x, z|\theta_1)$, and joint score $t(x, z|\theta_0) = \nabla_\theta \log\left(p(x, z|\theta)\right)\Big|_{\theta_0}$ can be computed for every event.
  [Brehmer, Kling, Espejo, Cranner (2019)]
- Uses loss functions that depend on $r(x, z|\theta_0, \theta_1)$ and $t(x, z|\theta_0)$, whose minimizing function is $r(x|\theta_0, \theta_1)$. [Brehmer, Louppe, Pavez, Cranmer (2018)]
- Projected sensitivities are then extracted through likelihood ratio tests.

Network architecture:

- 150 observables are used to describe the signal and background in the multivariate analysis.
- Fully connected NN with 3 hidden layers ($100 \times 100 \times 100$) is trained.

Projected sensitivity

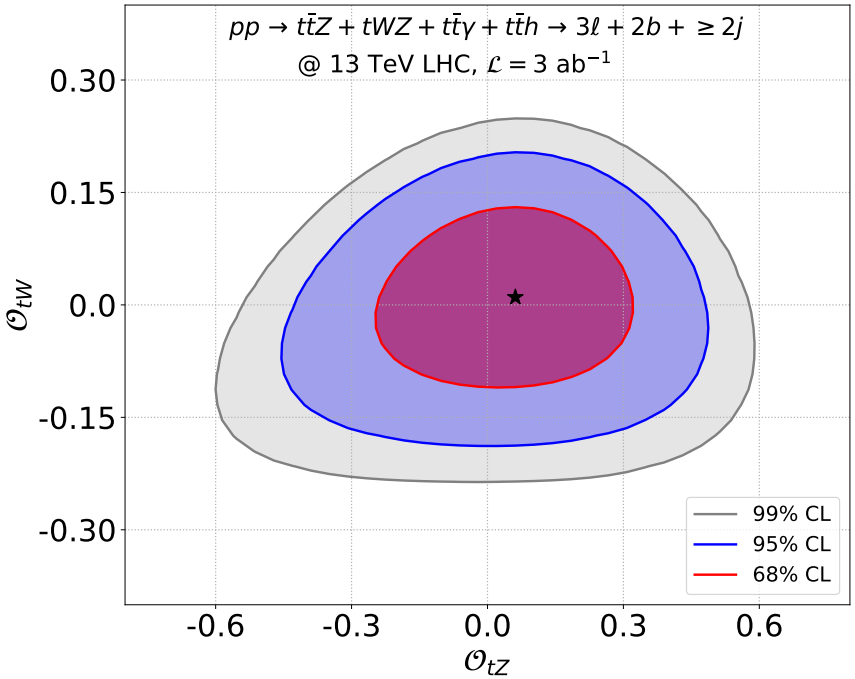

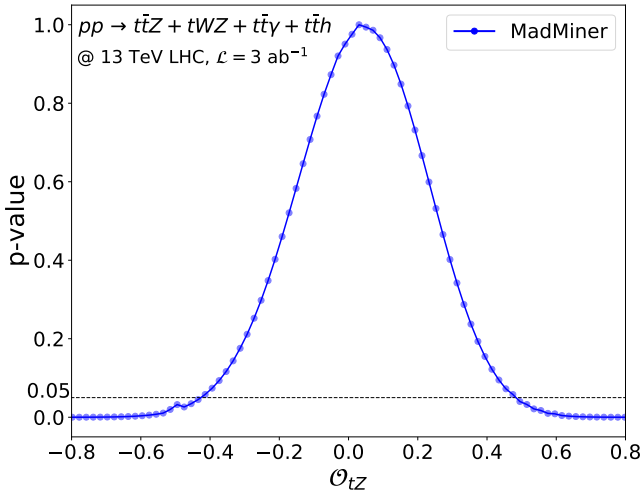

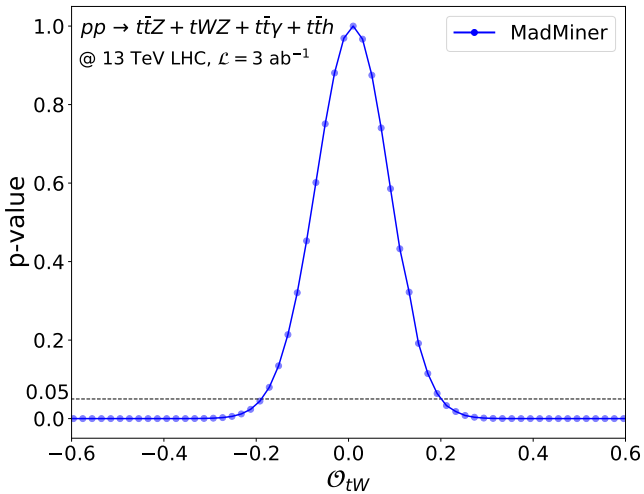

At 95% CL,
$\mathcal{C}_{tW} : [-0.18 : 0.18]$, $\mathcal{C}_{tZ} : [-0.41 : 0.47]$
At 68% CL,
$\mathcal{C}_{tW} : [-0.13 : 0.12]$, $\mathcal{C}_{tZ} : [-0.27 : 0.30]$

$pp \to tZj$ channel

- We focus on:
  $pp \to tZj \to (t \to \ell\nu b)(Z \to \ell\ell)j$
  $\to$ recent measurement of tZj cross-section at LHC at 4.2σ.

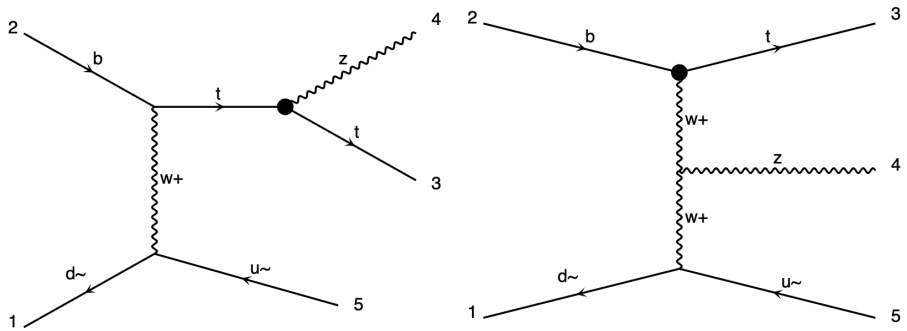

- Backgrounds: SM tZj, $t\bar{t}Z$, $WZ + jets$, tWZ, $t\bar{t}\gamma$, $t\bar{t}h$, VVV.
- NP modifications in $t\bar{t}Z$ and tWZ are also taken into account.

Event selection

- Final state: 3 ℓ + 1 b jets + 1/2 j.
- SFOS-ℓ pair with $m_{\ell\ell} = m_Z \pm 10$ GeV.
- Highest p_T jet associated with recoil jet.
- $\not{p}_z$ computed by constraining $m_{\ell_W \nu} = m_W$.
- top reconstructed by minimizing: $(m_{l_t \nu b} - m_t)^2 + (m_{l_t \nu} - m_W)^2$.

Reconstructed observables:

$$\theta^{\star W}_{\alpha}\{\alpha = \ell_W, \nu\}, \theta^{\star t}_{\beta}\{\beta = \ell_W, \nu, b\}, \theta^{\star tzj_{reco}}_{\epsilon}\{\epsilon = \ell_1, \ell_2, \ell_W, \nu, b, j_{reco}, t\},$$

$$p_{T,\zeta}, \eta_\zeta, \phi_\zeta, E_\zeta \ \{\zeta = \epsilon, Z, tZ, tZj_{reco}\}, m_k \ \{k = Z, t, tZ, tZj_{reco}\}, m_{\ell_1\ell_2\ell_W}, m^{\max}_{jj},$$

$$\Delta\phi_{\xi\rho} \ \{\xi = \ell_1, \ell_2, Z; \rho = \ell_W, b, j_{reco}\}, \Delta\phi_{\ell_W j_{reco}}, \Delta\phi^{tZj_{reco}}_{\ell_W Z}, \Delta\phi^{\max}_{\ell\ell} \ \{\ell = \ell_1, \ell_2, \ell_W\}, \Delta R^{\min}_{\ell b},$$

$$m_{T,l_W}, m_{T,tZ}, p^{\max}_{T,jj}, p_{T,jb}, p_{T,bj_{reco}}, H_T$$

Cut-based optimization

Several combinations of $\{H_T, m_{tZ}, p_{T,Z}, p_{T,W}, \Delta R_{t\ell}^{\min}, m_{jj}^{\max}, m_{tZ}, \Delta\eta_{Zb}, \Delta\eta_{bj_r}\}$ are tried.

$\mathcal{O}_{tZ}$: Cut-and-count analysis performed at $\{\mathcal{O}_{tZ} = \pm 0.5, \pm 1.0, \pm 1.5, \pm 2.0\}$.

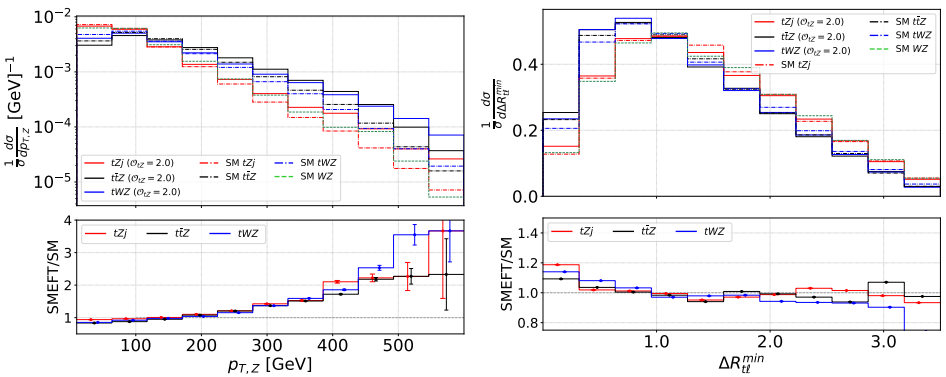

Event rates @ HL-LHC	$\mathcal{C}_{tZ} = 1.0$			$\mathcal{C}_{tZ} = -1.0$		
	$H_T >$ 450 GeV	$p_{T,Z} >$ 250 GeV	$\Delta R_{t\ell}^{min} <$ 2.75	$H_T >$ 350 GeV	$p_{T,Z} >$ 200 GeV	$\Delta\eta_{bj_r} <$ 4.75
SMEFT tZj	613	165	158	1260	313	289
SMEFT $t\bar{t}Z$	921	455	436	1696	774	771
SMEFT tWZ	118	45.3	43.3	207	80.6	80.1
tZj	584	139	132	1205	274	251
$t\bar{t}Z$	783	348	331	1519	653	648
tWZ	108	38.4	36.4	197	69.8	69.2
WZ	1497	367	337	2776	727	704
$t\bar{t}\gamma$	4.0	1.5	1.4	8.9	3.0	2.9
Significance	3.24	4.68	5.00	3.20	4.11	4.20

$\mathcal{O}_{tW}$: Cut-and-count analysis performed at $\{\mathcal{O}_{tW} = \pm 0.24, \pm 0.48, \pm 0.72\}$.

Event rates @ HL-LHC	$\mathcal{C}_{tW} = 0.48$		$\mathcal{C}_{tW} = -0.48$	
	$H_T >$ 200 GeV	$\Delta R_{t\ell}^{\min} <$ 3.25	$p_{T,Z} >$ 200 GeV	$\Delta R_{t\ell}^{\min} <$ 5.1
SMEFT tZj	3352	3275	2979	2770
SMEFT $t\bar{t}Z$	3414	3367	2499	2492
SMEFT tWZ	393	386	380	379
tZj	3038	2964	3159	2951
$t\bar{t}Z$	2881	2836	2887	2878
tWZ	368	362	370	368
WZ	6202	6022	6208	6036
$t\bar{t}\gamma$	20.1	19.8	20.8	20.7
Significance	7.80	7.84	4.96	5.03

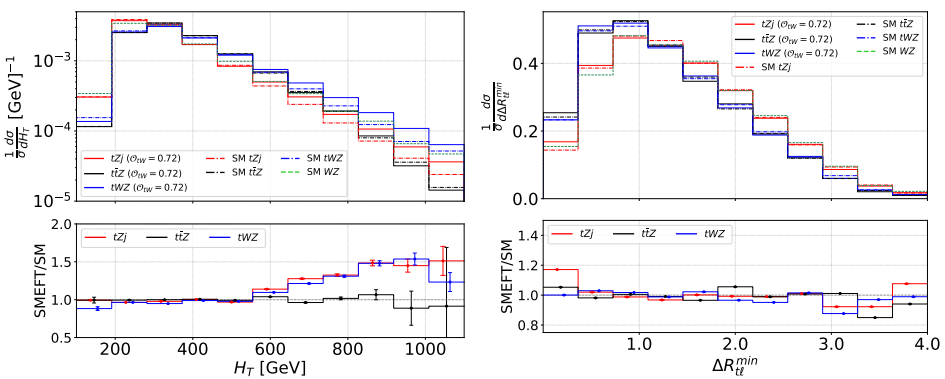

DNN

Two distinct NN's are trained:

- NN_{tZj}: Trained on EFT tZj and SM $t\bar{t}Z, tZj, WZ + jets$.
- $NN_{t\bar{t}Z}$: Trained on EFT $t\bar{t}Z$ and SM $t\bar{t}Z, tZj, WZ + jets$.

$\mathcal{C}_{tZ}$	NN	$S^{\star}_{SMEFT}(\alpha)$			$S^{\star}_{SM}(\alpha)$					α'	$\sigma_S^{NP\star}$
		tZj	$t\bar{t}Z$	tWZ	tZj	$t\bar{t}Z$	tWZ	WZ	$t\bar{t}\gamma$		
2.0	NN_{tZj}	287	140	16.0	177	65.8	9.9	244	0.4	0.63	18.3
	$NN_{t\bar{t}Z}$	143	1557	153	97.8	926	107.6	838	5.1	0.46	
1.0	NN_{tZj}	184	79.0	9.5	156	56.9	8.7	220	0.33	0.65	5.12
	$NN_{t\bar{t}Z}$	86.1	892	92.1	72.6	733	85.3	678	3.8	0.49	
-0.5	NN_{tZj}	619	214	27.5	601	202	26.7	819	1.3	0.47	1.44
	$NN_{t\bar{t}Z}$	280	1770	209	274	1700	208	1907	9.9	0.37	
-1.5	NN_{tZj}	282	153	17.2	203	94.7	12.1	255	0.5	0.59	11.21
	$NN_{t\bar{t}Z}$	152	1272	130	119	906	103	884	4.1	0.45	

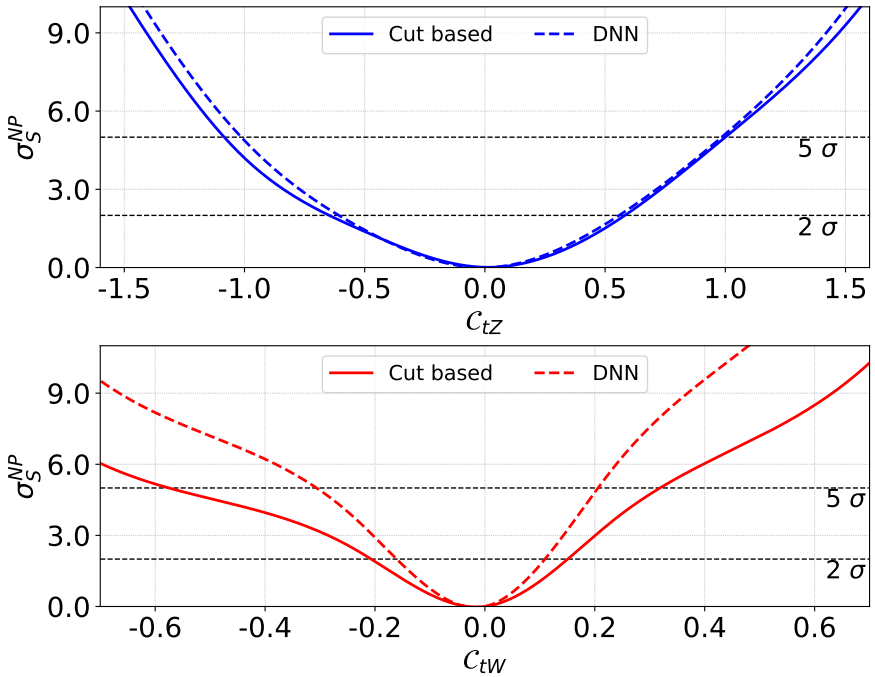

DNN

Two distinct NN's are trained:

- NN_{tZj}: Trained on EFT tZj and SM $t\bar{t}Z, tZj, WZ + jets$.
- $NN_{t\bar{t}Z}$: Trained on EFT $t\bar{t}Z$ and SM $t\bar{t}Z, tZj, WZ + jets$.

$\mathcal{C}_{tZ}$	NN	$S^{\star}_{SMEFT}(\alpha)$			$S^{\star}_{SM}(\alpha)$					α'	$\sigma_S^{NP\star}$
		tZj	$t\bar{t}Z$	tWZ	tZj	$t\bar{t}Z$	tWZ	WZ	$t\bar{t}\gamma$		
2.0	NN_{tZj}	287	140	16.0	177	65.8	9.9	244	0.4	0.63	18.3
	$NN_{t\bar{t}Z}$	143	1557	153	97.8	926	107.6	838	5.1	0.46	
1.0	NN_{tZj}	184	79.0	9.5	156	56.9	8.7	220	0.33	0.65	5.12
	$NN_{t\bar{t}Z}$	86.1	892	92.1	72.6	733	85.3	678	3.8	0.49	
-0.5	NN_{tZj}	619	214	27.5	601	202	26.7	819	1.3	0.47	1.44
	$NN_{t\bar{t}Z}$	280	1770	209	274	1700	208	1907	9.9	0.37	
-1.5	NN_{tZj}	282	153	17.2	203	94.7	12.1	255	0.5	0.59	11.21
	$NN_{t\bar{t}Z}$	152	1272	130	119	906	103	884	4.1	0.45	

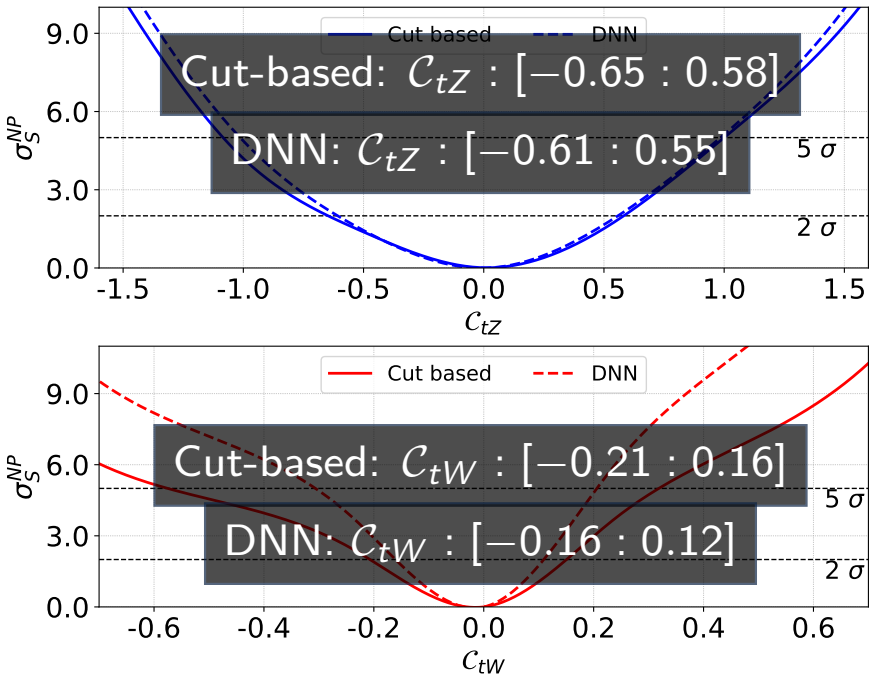

MadMiner

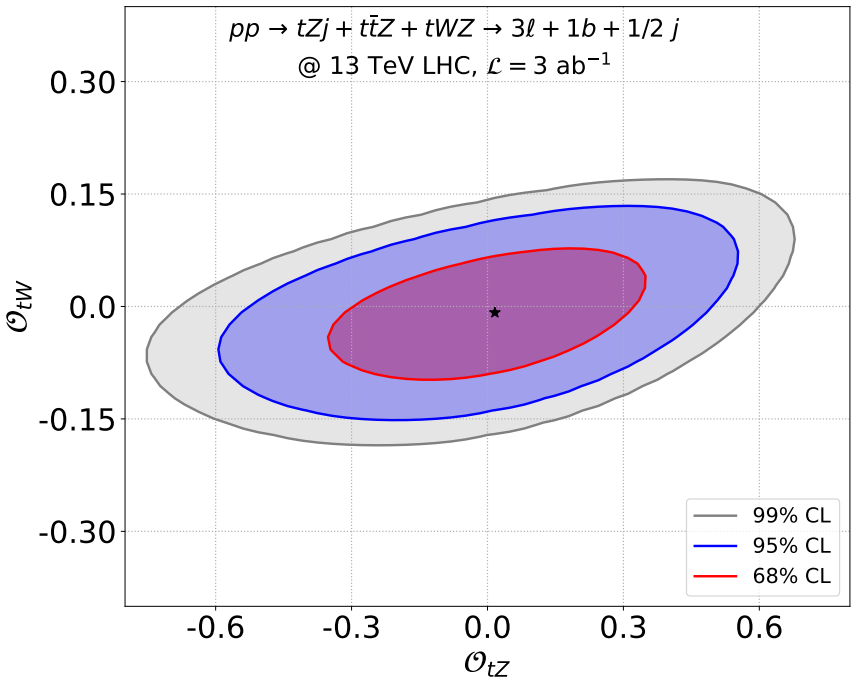

1-d profiling

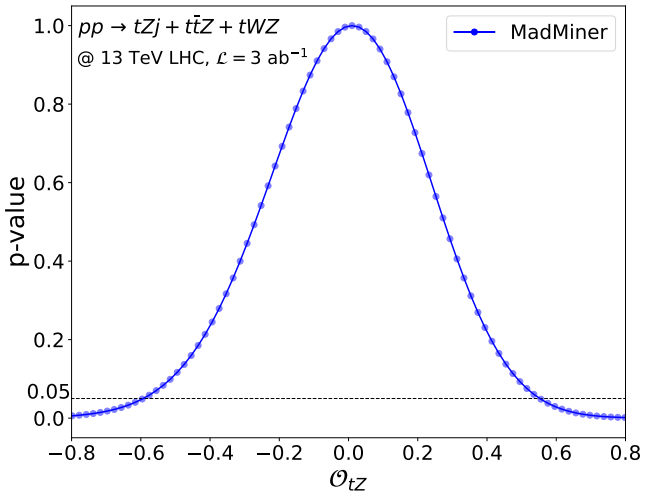

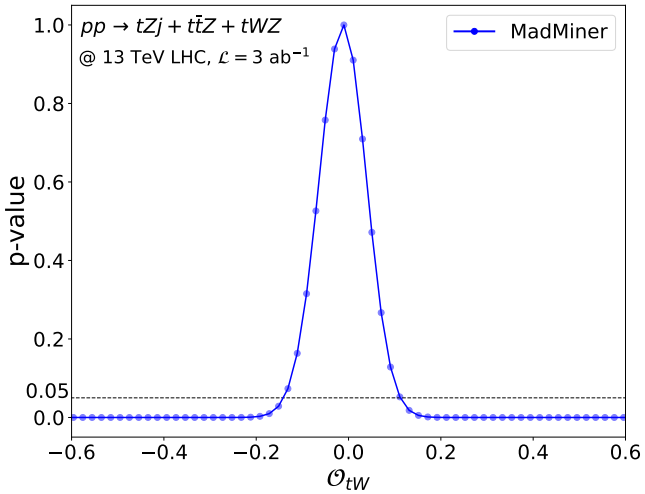

At 95% CL,
$\mathcal{C}_{tW} : [-0.14 : 0.11]$, $\mathcal{C}_{tZ} : [-0.59 : 0.55]$
At 68% CL,
$\mathcal{C}_{tW} : [-0.10 : 0.06]$, $\mathcal{C}_{tZ} : [-0.33 : 0.32]$

Summary of projected sensitivity

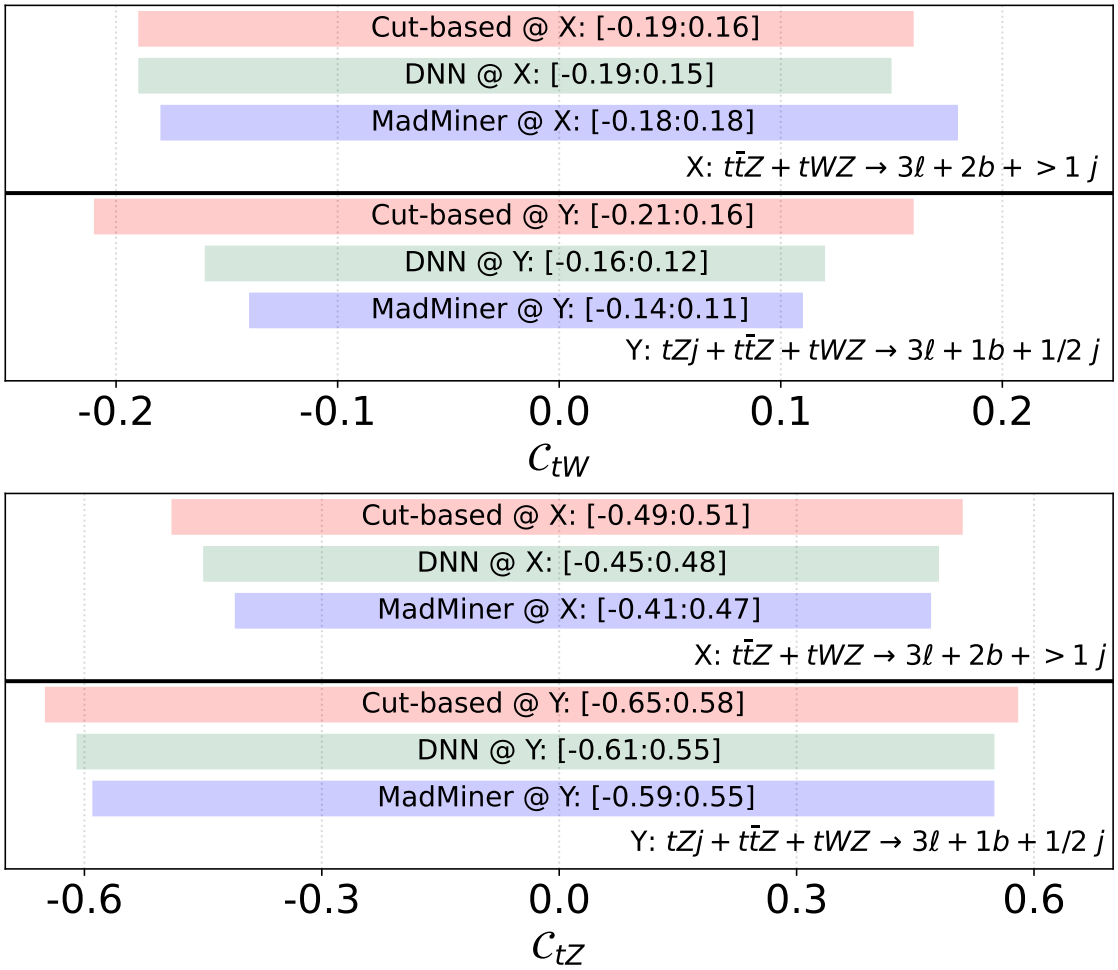

Projected 2σ sensitivity

Summary and outlook

- The upcoming high luminosity runs of LHC offer an exciting testbed to probe the rare top-quark production processes like tZj and $t\bar{t}Z$ with improved statistics.
- Opens up the possibility of measuring differential distributions of various kinematic observables.
- Complementing cross-section measurements with kinematic distributions can enhance the projected sensitivity for NP operators in tZj and $t\bar{t}Z$ processes.
- The inclusion of such differential measurements might also benefit the global-fit results.

Thank you for your attention!